The Plant Cell, Vol. 7, 2053–2067, December 1995

Immunocytological Localization of an Epitope-Tagged Plasma Membrane Proton Pump (H^+-ATPase) in Phloem Companion Cells

Natalie D. DeWitt[1] and Michael R. Sussman[2]

Cell and Molecular Biology Program and Department of Horticulture, University of Wisconsin, 1575 Linden Drive, Madison, Wisconsin 53706-1590

In higher plants, the plasma membrane proton pump (H^+-ATPase) is encoded by a surprisingly large multigene family whose members are expressed in different tissues. Using an 18-amino acid epitope tag derived from the animal oncogene c-Myc, we have performed immunocytolocalization measurements of the protein expressed by one member of this family, *AHA3* (Arabidopsis H^+-ATPase isoform 3). Immunofluorescence studies with tissue sections of transgenic plants have revealed that c-Myc-tagged AHA3 is restricted to the plasma membrane of phloem companion cells, whereas other AHA isoproteins are more widely distributed in the plasma membrane of other cell types. Electron microscopy with immunogold-labeled tissue sections suggests that there is a high concentration of proton pumps in the plasma membrane of companion cells but a much lower concentration in the plasma membrane of sieve elements. Due to plasmodesmata connecting the plasma membrane of these two adjacent cell types, it is likely that the proton motive force generated by the proton pump in companion cells can serve to power the uptake of sugar by proton-coupled symporters in either the companion cell or sieve element cell. The abundance of the proton pump in the plasma membrane of companion cells supports an apoplastic model for phloem loading in which the metabolic energy that drives sugar uptake is consumed by AHA3 at the companion cell plasma membrane. These experiments with a genetically altered integral plasma membrane protein demonstrate the utility of using a short c-Myc sequence as an epitope tag in Arabidopsis. Furthermore, our results demonstrate that, using genes encoding individual members of a gene family, it is possible to label plasma membrane proteins immunologically in specific, differentiated cell types of higher plants.

INTRODUCTION

Fick's Law predicts that over small distances (e.g., 1 to 2 mm), simple diffusion is sufficient for the movement of solutes necessary to support life. However, for transport over longer distances, multicellular organisms have evolved specialized structures to ensure that sugars and other solutes are supplied to cells far removed from nutrient sources. In higher plants, the phloem is a unique structure responsible for long-distance movement of sugars, hormones, and other nutrients. Within the phloem vasculature are two anatomically distinct cell types, the sieve tube element and the companion cell. Although these two contiguous cells originate by unequal cell division of a common mother cell, their morphologies are strikingly distinct and suggest that each performs unique physiological functions (Evert, 1990). The presence of a nucleus and the abundance of organelles and ribosomes in the companion cell suggest that this cell is active in protein synthesis and metabolism. In contrast, the scarcity of organelles within the sieve elements and the presence of sieve plate pores in the cross walls between each column of cells appear to be specializations that allow rapid and massive movement of sugars and other solutes. Whereas the morphological differences between sieve tube cells and companion cells imply differences in their respective transport functions, little or no cytochemical or biochemical data exist on the structure and function of specific plasma membrane transport proteins residing in each cell type.

The primary active transport system at the plasma membrane of plants is a P-type proton pump (H^+-ATPase), which generates the proton motive force used to drive the uptake and accumulation of solutes within each cell (for example, see Bush, 1993). Many plant genes have been cloned encoding proteins with structural characteristics of P-type cation-translocating ATPases, a family of proteins also found in fungi, bacteria, and animals. These proteins couple ATP hydrolysis to ion translocation, thereby generating ion gradients across cellular membranes and maintaining the osmotic and chemical balance

[1] Current address: Biology Department, The Plant Laboratory, University of York, Heslington, York, Y01 5DD, England.
[2] To whom correspondence should be addressed.

of the cytoplasm. At least 10 genes encoding P-type ATPases have been identified in Arabidopsis, and based on identity with amino acid sequence derived from the purified enzyme, these were predicted to encode plasma membrane proton pumps (H^+-ATPases) (Harper et al., 1989, 1994; Pardo and Serrano, 1989; Serrano, 1989; Sussman, 1994). Using a yeast expression system, this prediction was recently confirmed for several H^+-ATPase isoforms (Palmgren and Christensen, 1993, 1994).

The experiments performed in this study were prompted by our previous reporter gene studies of one of 10 genes encoding the Arabidopsis plasma membrane H^+-ATPase. These experiments demonstrated that the promoter for *AHA3* (Arabidopsis H^+-ATPase isoform 3) drives reporter gene expression only in cells within the phloem of vegetative tissue, which suggested that we had identified the proton pump providing the driving force for loading solutes into the phloem (DeWitt et al., 1991). Similar studies with upstream sequences of three other gene isoforms, *AHA10*, *AHA2*, and *AHA9*, reveal different expression patterns, with the *AHA10* promoter directing expression only in cells of the seed integument (Harper et al., 1994), *AHA2* in the root epidermis and cortex (J.F. Harper, unpublished results), and *AHA9* in the anthers of transgenic tobacco (Houlné and Boutry, 1994).

Whereas our previous study of the *AHA3* gene promoter raised the possibility that the biochemical properties of the AHA3 protein are uniquely suited to providing energy for phloem loading and translocation, an immunological approach that distinguished AHA3 from the other isoproteins was required to test this hypothesis directly. Here, we describe AHA3-specific immunolocalization studies, using the *AHA3* gene tagged with sequences encoding a c-Myc epitope, to distinguish it immunologically from other highly conserved AHA isoproteins. Immunofluorescence in tissue sections of transgenic plants revealed that expression of the c-Myc–tagged AHA3 polypeptide is restricted to phloem companion cells and not sieve elements or parenchyma cells. In contrast, other H^+-ATPase isoproteins were more generally distributed in nonphloem cell types, and within the phloem, these isoproteins were found in phloem parenchyma cells in addition to companion cells. c-Myc was shown to be an appropriate epitope tag for Arabidopsis immunocytochemistry because there was little or no background immunoreactivity in wild-type plants. We also used immunogold labeling to determine quantitatively that H^+-ATPases are much more abundant in the plasma membrane of companion cells than in sieve elements, which appear to be virtually devoid of H^+-ATPases.

RESULTS

A plant expression plasmid vector was constructed containing 5 kb of *AHA3*-transcribed genomic sequence, 4 kb of 5′ upstream sequence, and 2.3 kb of downstream sequences. Using site-directed mutagenesis, BamHI sites were inserted into one of two separate sites in the C-terminal coding sequences, corresponding to cytoplasmically located amino acids 904 and 944 (Figure 1A). The nucleotide sequence encoding a 14–amino acid c-Myc epitope (Kolodziej and Young, 1991) was translationally fused to a genomic clone encoding AHA3 (Figure 1B). The two different modified *AHA3* genes were cloned into an Agrobacterium binary plasmid, and at least six independently transformed kanamycin-resistant Arabidopsis plants were generated with each plasmid. Results shown are typical of the transgene present in multiple transgenic plant lines and thus are independent of the chromosomal location of the transgene.

As a first test of whether the epitope-tagged AHA3 protein was expressed, microsomes were prepared from crude extracts of transgenic plant lines transformed with the construct encoding AHA3 with an epitope inserted at either amino acid position 904 or 944. SDS-PAGE and immunoblot analyses were performed using commercially available monoclonal antibodies generated against the c-Myc epitope. As shown in Figure 2A,

A

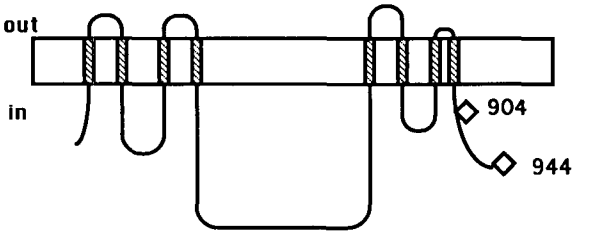

B

AHA3:	GGYRE**LS**	EI
904/myc:	GGYRE**DPPEQKLISEEDLLDP**EI	
AHA3:	DIETA**G**	HYTV
944/myc:	DIETA**DPPEQKLISEEDLLDPHRLIKI**	

Figure 1. Location and Structure of the c-Myc Epitope Tag within the Plasma Membrane Proton Pump (H^+-ATPase).

(A) A model for the predicted topological structure of the *AHA3*-encoded protein, based on a computer-assisted hydropathy plot. Open diamonds denote the two positions at the C terminus, either amino acid 904 or 944, where the epitope was inserted.

(B) Amino acid sequence of the c-Myc epitope. AHA3 residues deleted in the epitope-tagged proteins are shown in boldface, as are AHA3–c-Myc residues that are additions or substitutions to the wild-type sequence. Amino acids encoding the c-Myc epitope are underscored.

there was little or no wild-type protein reactive with the anti–c-Myc antibody in wild-type membranes. In contrast, in membranes from transgenic plants expressing either of the two c-Myc–tagged ATPases, a strong c-Myc immunoreactive band was observed at 100 kD, the predicted molecular mass for the H+-ATPase.

Interestingly, the 944–c-Myc protein ran as a single band, whereas the 904–c-Myc protein ran as a doublet. This pattern, which was consistently and reproducibly observed with extracts from independent transgenic lines, is probably due to proteolysis of the more C-terminal 944 epitope. Thus, a proteolyzed 944 protein would be undetectable with the anti–c-Myc antibody, whereas both the proteolyzed and intact forms of the 904 c-Myc would be evident and appear as a doublet. Based on this immunoblot result, it is likely that a proteolytic cleavage site exists between amino acids 904 and 944.

The identity of this protein as the plasma membrane proton pump was confirmed by stripping the epitope antibody from these blots and reprobing with a polyclonal antibody directed against the C terminus of AHA2 (DeWitt, 1994). An immunoblot using this polyclonal anti–H+-ATPase antibody to probe Arabidopsis microsomal proteins is shown in Figure 2B. The AHA2 isoform was previously shown to be expressed predominantly in roots (Harper et al., 1990), but structural similarities between the C termini of the known members of the *AHA* gene family (see Harper et al., 1994; Sussman, 1994) suggest that most or all AHA isoforms are recognized by this antibody. For example, comparison of the C-terminal 102 amino acids of AHA2 with AHA1 and AHA3 shows 87 and 80% amino acid identity, respectively. The high immunoreactivity of this AHA2-derived antibody with AHA3 was experimentally verified by immunoblotting a 160-kD AHA3/β-glucuronidase chimeric protein (DeWitt, 1994).

Using indirect immunofluorescence, the cellular and subcellular localization of AHA3–c-Myc was determined in leaf and stem transections. Leaf sections of plants expressing AHA3–c-Myc (904 and 944) displayed highly specific labeling of a discrete population of phloem cells in both major and minor veins (Figures 3A to 3C). The cells were labeled predominantly at their periphery such that they had a "halo" appearance, consistent with plasma membrane labeling. Leaf sections of untransformed wild-type control plants displayed no labeling (Figure 3D), confirming that the staining observed in AHA3–c-Myc–transformed plants is specific for the c-Myc–tagged AHA3 protein. Similarly, no labeling of freehand stem sections from wild-type plants was observed using anti–c-Myc sera (Figure 4A), whereas stem sections of plants transformed with AHA3–c-Myc strongly and specifically labeled a discrete population of cells in the phloem (Figure 4B). Multiple lines of the 904- and 944-tagged constructs were tested, and all displayed this staining pattern.

The cells specifically labeled by the anti–c-Myc sera were identified as phloem companion cells, based on the size, arrangement, cytoplasmic density, and contents of different phloem cells. Most strikingly, the labeled cells contained dense

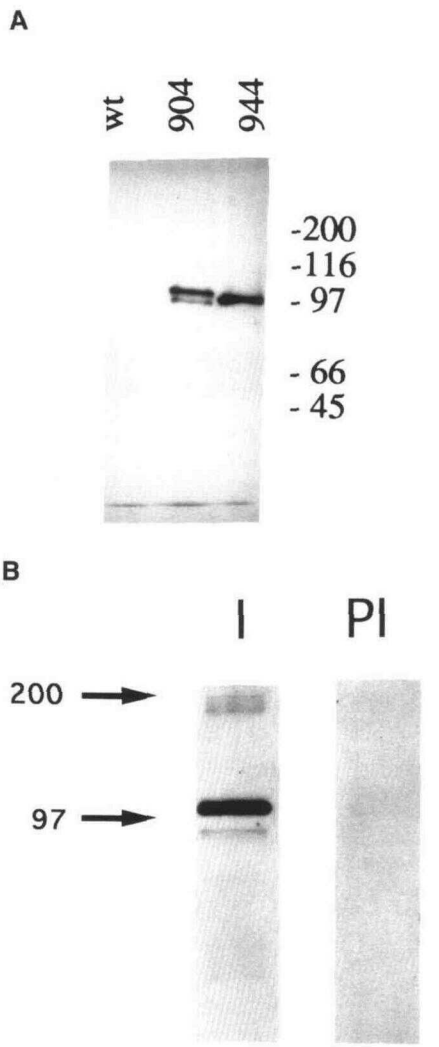

Figure 2. SDS-PAGE Immunoblots of Membranes from Wild-Type and Transgenic Plants.

(A) Immunoblot of AHA3–c-Myc. Microsomal proteins (60 μg) from untransformed control plants (WT) and from AHA3–c-Myc–expressing transgenic plants, with AHA3 tagged at either amino acid 904 or amino acid 944. Proteins were immunoreacted with the anti–c-Myc monoclonal antibody designated 9E10.2. Molecular weight in kilodaltons is indicated at right.

(B) Immunoblot of wild-type H+-ATPase. Microsomal proteins (15 μg) from wild-type plants immunoreacted with anti–H+-ATPase sera (I) or preimmune serum (PI). Molecular weight in kilodaltons is indicated at left.

cytoplasm and chloroplasts, which are characteristics of companion cells rather than sieve elements. Confocal microscopy confirmed that chloroplast autofluorescence appeared within the same focal plane as the c-Myc immunofluorescent label, and thus, chloroplasts were contained within labeled cells rather than beneath them (data not shown). Special care was

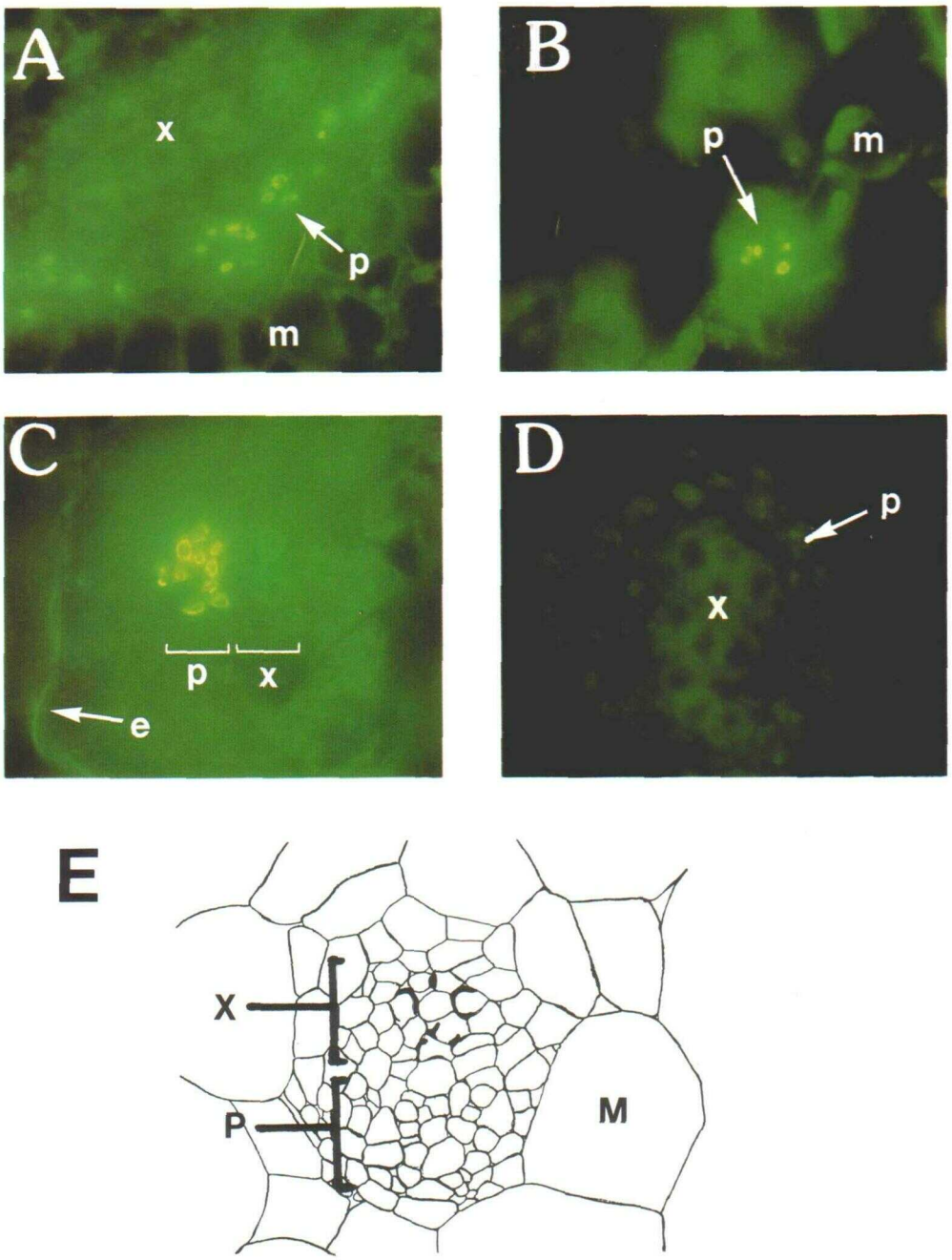

Figure 3. Anti–c-Myc Labeling of Leaf Veins in Plants Expressing AHA3–c-Myc.

Frozen cryostat sections (8 μm) were labeled with anti–c-Myc monoclonal mouse antibody and FITC-conjugated anti–mouse IgG_1 sera.
(A) to **(C)** show labeling of vein transections from Arabidopsis expressing AHA3–c-Myc, and **(D)** shows labeling of vein transection from untransformed control Arabidopsis. Bar in **(C)** (labeled p) indicates 15 μm and applies to all panels.
(A) Major vein transection showing labeling in a subset of phloem cells (p) but not xylem (x) and mesophyll (m) cells.
(B) Minor vein transection showing labeling in a subset of phloem cells (p) but not xylem (unlabeled) or mesophyll (m) cells.
(C) Intermediate vein transection showing labeling in a subset of phloem cells (p) but not xylem (x), mesophyll (unlabeled), or epidermal (e) cells.
(D) Major vein transection showing absence of labeling in phloem (p) cells of untransformed control plants. Autofluorescence from xylem (x) is visible as a dark green background.
(E) Schematic drawing of the transection of an Arabidopsis major vein, with a mesophyll cell (m), and xylem (x) and phloem (p) tissues labeled.

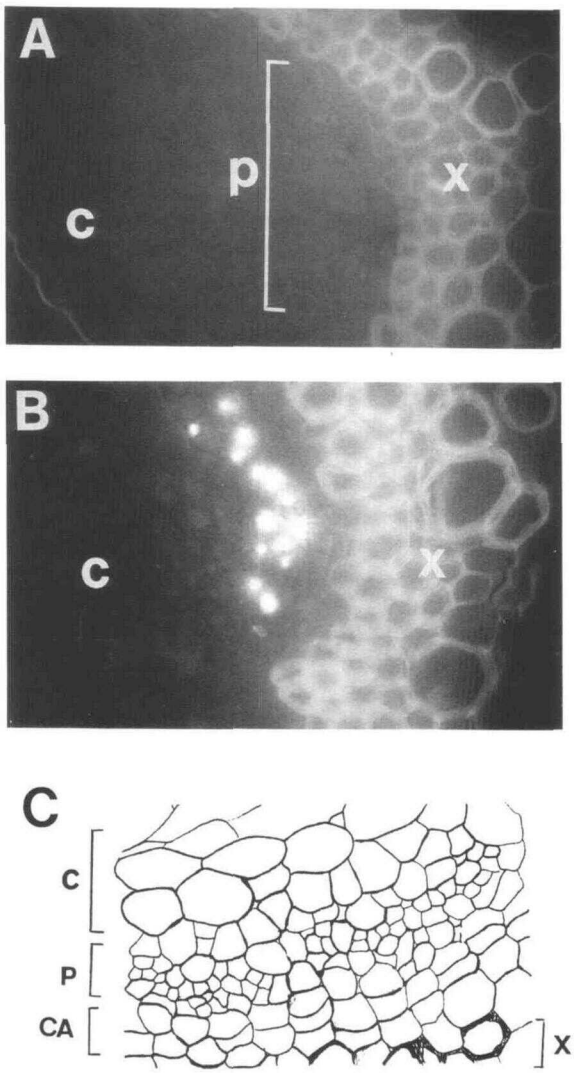

Figure 4. Anti–c-Myc Labeling of a Stem Cross-Section in Plants Expressing AHA3–c-Myc.

Stem transections (free hand) were labeled with anti–c-Myc mouse monoclonal antibodies and FITC-conjugated anti–mouse IgG_1 sera. In **(A)**, the bar labeled p indicates 25 μm and applies to both **(A)** and **(B)**.
(A) Labeling of stem transection from untransformed control Arabidopsis. Cortical (c) and phloem (p) cells show no labeling, and xylem (x) shows only autofluorescence.
(B) Stem transection from Arabidopsis expressing AHA3–c-Myc, showing intense, cell-specific labeling in a subset of phloem cells but not cortical (c) or xylem (x) cells.
(C) Schematic drawing of a vein transection from an Arabidopsis stem, with the cortex (C), phloem (P), xylem (X), and cambium (CA) labeled.

taken to assess labeling of phloem parenchyma cells, which, based on their "transfer cell" morphology suggestive of membrane transport function (DeWitt, 1994), might be expected to express high levels of H+-ATPase (although not necessarily AHA3). However, under our labeling and plant growth conditions, anti–c-Myc labeling of phloem parenchyma transferlike cells in leaves was not observed.

A trivial explanation for the absence of labeling in non-companion cells is that the other cell types are not as accessible to antibodies under these labeling conditions. To address this possibility, cells were labeled with anti-actin sera. Examination of stained leaf sections using confocal microscopy revealed that anti–c-Myc sera predominantly labeled the cell periphery. In contrast, anti-actin label was distributed throughout the cytoplasm, although it sometimes appeared concentrated near organelles or at the plasma membrane (DeWitt, 1994). Moreover, anti-actin sera labeled nearly all cells of the vein as well as some adjacent mesophyll cells. Phloem parenchyma and mesophyll cells must therefore be accessible to antibodies in this procedure, in support of our conclusion that AHA3–c-Myc localization is restricted to companion cell plasma membranes.

A more rigorous means of identifying cell types within the phloem is electron microscopy using immunogold-labeled sections. Unfortunately, immunogold studies with Lowicryl-embedded ultrathin sections from transgenic plants did not provide significant labeling with anti–c-Myc monoclonal antibodies, perhaps because of fixation conditions that reduced immunoreactivity of the epitopes or resin-embedding procedures that masked the epitopes. However, using the polyclonal antibody directed against all AHA isoforms and mild fixation conditions, we were able to observe significant immunogold labeling of the plasma membrane in companion cells. In these experiments, the structure of Arabidopsis stem and leaf veins was first examined under optimal fixation conditions using electron microscopy to identify the arrangement of cell types within the phloem and to determine their size and contents. Figure 5 shows a typical companion cell–sieve element complex from an Arabidopsis bolting stem fixed for standard transmission electron microscopy. In stems, the companion cells are usually equal to or smaller in size than sieve elements and contain strikingly dense cytoplasmic ground material, numerous mitochondria, chloroplasts, and large vacuoles. In contrast, sieve elements are devoid of most organelles and cytoplasmic ground material but contain starch granules and a parietal arrangement of smooth endoplasmic reticulum, mitochondria, and plastids (see DeWitt, 1994, for a more detailed description of Arabidopsis phloem cell ultrastructure).

Lowicryl-embedded stem sections were labeled with anti–H+-ATPase sera, and electron microscopy revealed that immunogold label was concentrated on the plasma membrane of companion cells, with little or no labeling of sieve elements (Figure 6). In plasmolyzed cells, the immunogold label clearly followed the contours of the plasma membrane and was not associated with the cell wall. Companion cell–sieve element complexes were randomly selected and photographed, and their plasma membrane–associated gold particles were counted. On average, companion cells contained 1.7 gold particles per micrometer of plasma membrane, whereas sieve elements contained 0.2 gold particles per micrometer of plasma membrane, an amount that is not significantly different from the background (Figure 7). Because of technical limitations,

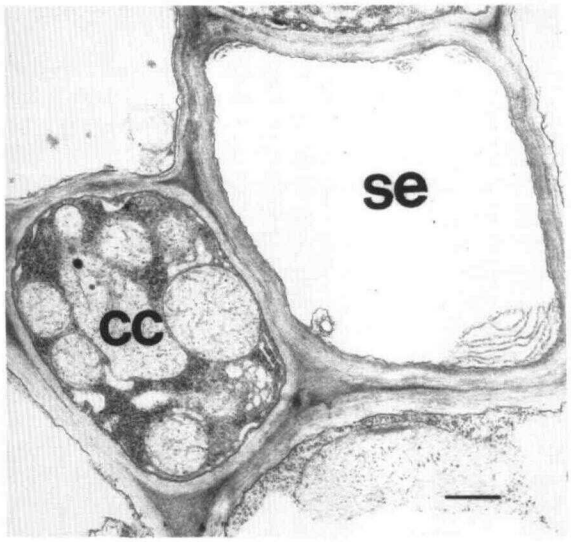

Figure 5. Companion Cell–Sieve Element Complex in Transection of Arabidopsis Bolting Stem.

The cytoplasm visible in the companion cell (cc) is extremely dense and contains numerous mitochondria and other organelles. The sieve element (se) is devoid of most organelles but contains fibrillar P-protein and a parietal layer of smooth endoplasmic reticulum. Bar = 1 μm.

such as inaccessibility of antigen to antibodies and potential clustering of primary and secondary antibodies, these values probably reflect the relative levels of H^+-ATPase in companion cells and sieve elements rather than absolute concentrations of H^+-ATPase in the plasma membrane.

Fixation conditions that yielded the best cellular preservation (i.e., glutaraldehyde–paraformaldehyde mixtures) yielded low signal and high nonspecific labeling. Difficulties were previously reported in localizing yeast H^+-ATPases using immunogold labeling with antisera against the C terminus (Monk et al., 1991). Epitope mapping experiments confirmed that the yeast C terminus had low antigenicity (Serrano et al., 1993), presumably because the conformational configuration of the C terminus impedes antibody–antigen recognition. The phloem H^+-ATPase localized in this study was also sensitive to fixation and resin embedding, perhaps because of similar properties. Despite the suboptimal ultrastructural preservation, this analysis did confirm that H^+-ATPases are abundant in companion cells and virtually undetectable in sieve elements and that most of the labeling in companion cells is concentrated on the plasma membrane. These results are in general agreement with those of Bouche-Pillon et al. (1994), who, using an ATPase polyclonal antibody with ultrathin sections of *Vicia faba* minor veins, observed many immunogold particles on the plasma membrane of phloem transfer cells but few on the plasma membrane of sieve tubes.

Our electron microscopic studies were especially useful for evaluating results from light microscopic immunofluorescence studies, in which we compared the "general" H^+-ATPase distribution with the epitope-tagged AHA3 distribution. Parallel immunofluorescence experiments with the anti–H^+-ATPase polyclonal sera demonstrated labeling of multiple cell types (Figures 8A to 8I), in contrast to specific labeling of companion cells by anti–c-Myc sera shown in Figures 3 and 4. In stem sections (Figures 8A to 8F), companion cells and guard cells were labeled most intensely, followed by phloem parenchyma, xylem parenchyma, cortical, and cambial cells. Little labeling was observed in pith cells and sieve elements, and no labeling was observed in tracheary elements, consistent with the absence of plasma membrane in those structures. In leaf sections (Figures 8G to 8I), numerous cell types were also labeled: guard cells, companion cells, phloem parenchyma, vascular parenchyma, and mesophyll. In most cells, the plasma membrane was predominantly labeled, although nonspecific labeling was sometimes observed on chloroplasts.

Double-labeled immunofluorescence was used to compare more directly the distribution of AHA3–c-Myc with that of other AHAs present in leaves and stems, as shown in Figures 9A to 9C. Anti–c-Myc and anti–H^+-ATPase sera were individually or simultaneously applied to sections and visualized with rhodamine red–conjugated and fluorescein isothiocyanate (FITC)–conjugated secondary antibodies, respectively. Cells labeled by anti–H^+-ATPase appeared green, cells labeled by anti–c-Myc appeared red, and cells labeled by both antisera appeared yellow-orange. When sections were treated with anti–H^+-ATPase sera only and viewed with the double-band pass filter, only green fluorescence was observed (Figure 9A). When sections were treated with anti–c-Myc sera only and viewed with the double-band pass filter, only red fluorescence was observed (data not shown). When sections were treated with both sera and viewed with the double-band pass filter, both green and yellow-orange fluorescence was observed (Figure 9B), indicating that both sera labeled a subset of cells and that anti–H^+-ATPase sera labeled the remainder of cells.

We determined that overlap in labeling between the anti–c-Myc and anti–H^+-ATPase antibodies occurs exclusively in companion cells. In stem sections labeled only with anti–H^+-ATPase sera, companion cells as well as cortical, cambial, and phloem parenchyma cells appeared green (Figure 9A). However, in stems from plants expressing AHA3–c-Myc labeled with both anti–H^+-ATPase and anti–c-Myc, cortical, cambial and phloem parenchyma cells appeared green, whereas only companion cells appeared yellow-orange (Figure 9B). Thus, companion cells are labeled by both antisera, whereas the other cell types are labeled exclusively by anti–H^+-ATPase sera. In comparisons of double-labeled companion cells and guard cells, companion cells again were labeled by both sera, whereas guard cells were labeled only by anti–H^+-ATPase sera (DeWitt, 1994).

To reduce the glare from chloroplast autofluorescence when using the double-band pass filter, it was sometimes necessary to make adjustments that reduced the anti–c-Myc signal such that in these figures it appears weaker than the anti–H^+-ATPase signal. However, for the following reasons, the speci-

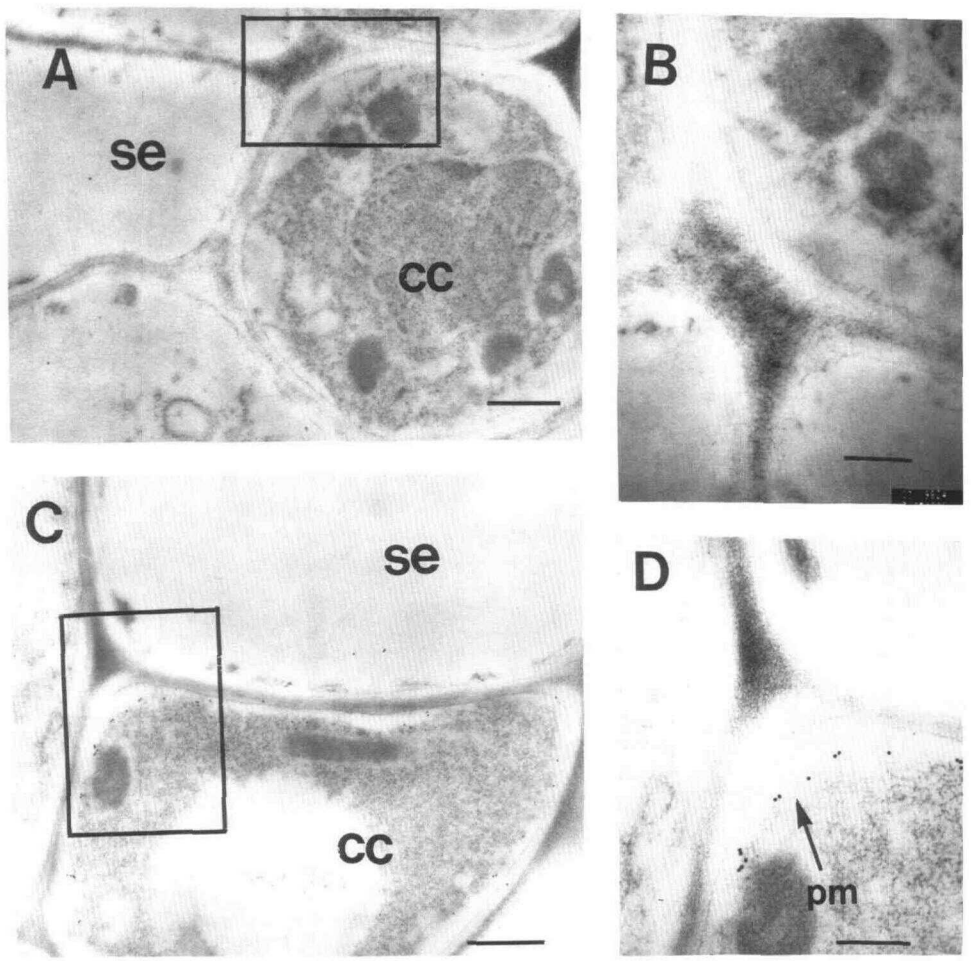

Figure 6. Immunogold Localization of H+-ATPases in Arabidopsis Stem Companion Cell–Sieve Element Complexes.

(A) Control in which the transection was treated with preimmune sera and gold-conjugated secondary antibody. Note the absence of gold particles on the companion cell (cc) plasma membrane. se, sieve element. Bar = 0.5 μm.

(B) Higher magnification of boxed region in **(A)**, showing absence of gold particles in the plasma membrane of companion and adjacent cells. Bar = 0.5 μm.

(C) Transection treated with anti–H+-ATPase sera and immunogold-conjugated secondary antibody, showing gold particles on plasma membrane of companion cells (cc) but not sieve elements (se). Bar = 0.5 μm.

(D) Higher magnification of boxed region in **(C)**, showing gold particles on the plasma membrane (pm) of companion cells but not adjacent phloem parenchyma or sieve elements. Bar = 0.5 μm.

ficity of companion cell labeling is not an artifact resulting from weak anti–c-Myc labeling. First, the double-labeling experiments were conducted using different combinations of antibodies and fluorochromes, and the same results were observed, that is, anti–c-Myc labeled companion cells only, whereas anti–H+-ATPase labeled multiple cell types. Second, under identical imaging conditions, anti–c-Myc labeling of companion cells gave an intensity equal to the anti–H+-ATPase labeling of companion cells without labeling of any other cell type.

As a final confirmation that sieve elements contained undetectable amounts of c-Myc–tagged AHA3, we also performed double-labeling experiments with a recently derived monoclonal antibody directed against a sieve element–specific isoform of β-amylase (Wang et al., 1995). This antibody, designated RS5, was visualized with a secondary antibody coupled to the red fluorochrome rhodamine, whereas the anti–c-Myc monoclonal antibody was visualized with a secondary antibody coupled to the green fluorochrome FITC. An image at the excitation wavelength corresponding to each fluorochrome was collected using a laser confocal microscope in the dual channel mode (568 nm for rhodamine and 488 nm for FITC), and after digitization and merging, pseudocolors denoting rhodamine as red and FITC as green were assigned, and contrast

was enhanced using the BioRad Cosmos imaging program. As shown in Figure 9D, adjacent cells were labeled with either red or green fluorochromes, and no cells were observed containing both colors. Taken together, these results demonstrate that the expression of c-Myc–labeled AHA3 is restricted to companion cells within the phloem.

DISCUSSION

The measurement of plasma membrane H^+-ATPase content has been the object of many studies on the relative transport capacities of various plant cells. For example, mechanisms and sites of phloem loading were inferred by cytochemical determinations of the ATPase, but these studies were subsequently shown to localize a cell wall phosphatase rather than a cation-pumping ATPase (Katz et al., 1988). More recently, light microscopic immunolocalization studies using polyclonal antisera raised against purified H^+-ATPase have demonstrated the abundance of H^+-ATPases in guard cells, phloem cells, pollen grains, and root epidermis, pericycle, xylem parenchyma, and endodermis. These studies used antisera raised against undefined H^+-ATPase epitopes from preparations of heterogeneous 100-kD proteins (Samuels et al., 1992),

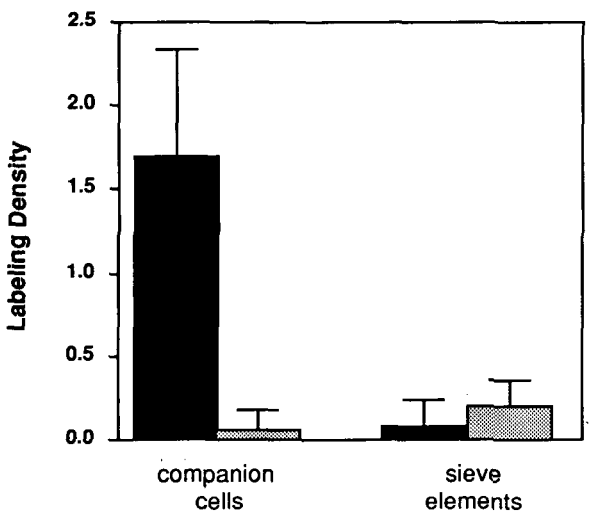

Figure 7. Comparison of the Density of Immunogold Labeling in the Plasma Membrane of Companion Cells versus Sieve Elements.

Electron microscopy was used to count gold particles localized on the plasma membrane of companion cells and sieve elements in Arabidopsis Lowicryl-embedded stem sections, labeled with anti-H^+-ATPase immune (solid bars) and preimmune (stippled bars) sera. Labeling density is expressed as number of gold particles per micrometer of plasma membrane. For immune sera data, 57 companion cells and 54 sieve elements were analyzed, and for preimmune sera data, seven companion cells and seven sieve elements were analyzed. Error bars indicate the standard error.

plasma membrane preparations from corn coleoptiles (Villalba et al., 1991; Obermeyer et al., 1992; Stenz et al., 1993), and an AHA3 C-terminal fusion protein (Parets-Soler et al., 1990; Bouche-Pillon et al., 1994).

It is now recognized that plant plasma membrane H^+-ATPases are encoded by surprisingly large multigene families (Boutry et al., 1989; Ewing et al., 1990; Harper et al., 1990, 1994), and thus, the previous immunolocalization studies failed to distinguish between different H^+-ATPase isoproteins. Molecular biological analyses show that individual members of the H^+-ATPase multigene family are subject to differential temporal and spatial gene regulation (Boutry et al., 1989; Harper et al., 1990; DeWitt et al., 1991; Ewing and Bennett, 1994) and encode isoproteins with different kinetic and regulatory properties (Palmgren and Christensen, 1994). Therefore, correlating the cellular localization of each H^+-ATPase isoprotein with its regulatory and kinetic properties will provide the most meaningful view of how active transport relates to cellular function. With this goal in mind, the expression of an individual AHA isoprotein, AHA3, was examined in Arabidopsis vascular cells, and its expression was compared with the "total" plasma membrane H^+-ATPase content of these and other cell types.

First, we discuss the distribution of total H^+-ATPases or, more specifically, those recognized by the anti-H^+-ATPase polyclonal sera. This antisera was raised against a fusion of the C terminus of AHA2 protein with glutathione-*S*-transferase (N.D. DeWitt, M.R. Sussman, and J.F. Harper, unpublished data). Because of the high sequence identity in this region of the protein among AHAs, we propose that this antibody recognizes many or all AHA isoproteins. Using this antibody, we observed that guard cells and phloem cells contained high concentrations of the plasma membrane H^+-ATPase, as reported previously (Parets-Soler et al., 1990; Villalba et al., 1991; Samuels et al., 1992; Bouche-Pillon et al., 1994). Because of the increased sensitivity of our method (immunofluorescence of unembedded tissue), significant levels of H^+-ATPase were found in several previously unreported cell types, including cambial, vascular parenchyma, cortical, and trichome cells. In general, H^+-ATPase content appeared to vary, depending on the cell's presumed transport activity, specified by its developmental stage or the position it occupies in the path of solute transport.

In contrast to the widespread distribution of plasma membrane H^+-ATPases, using an epitope tag technique, AHA3 was found to be specifically localized in phloem cells. Immunofluorescence studies demonstrated that the cells within phloem that were labeled intensely with an anti-c-Myc monoclonal antibody are companion cells and not sieve elements or phloem parenchyma cells. In marked contrast to phloem companion cells, the adjacent sieve elements contained virtually undetectable levels of AHA3 or other H^+-ATPases, as demonstrated by both immunogold- and immunofluorescent-labeling techniques. It is possible that sieve elements contain a highly diverged H^+-ATPase isoprotein that is unrecognized by the anti-H^+-ATPase sera used in this study. More likely, this

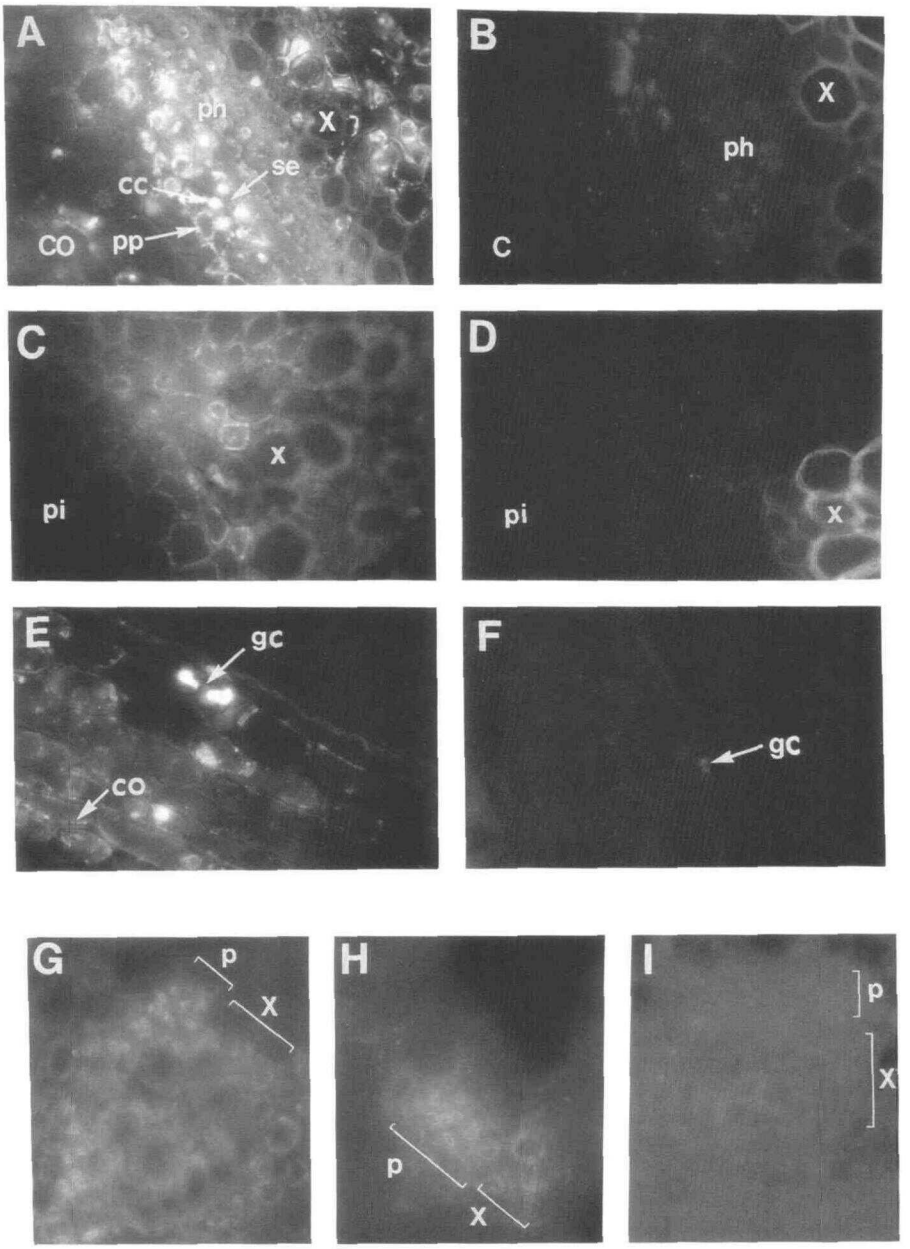

Figure 8. Distribution of H⁺-ATPases in Arabidopsis Stem Vascular Bundles and Leaf Veins.

Stem transections were labeled with either anti–H⁺-ATPase immune sera shown in **(A)**, **(C)**, **(E)**, **(G)**, and **(H)** or with preimmune sera shown in **(B)**, **(D)**, **(F)**, and **(I)** and detected with FITC-conjugated secondary antisera. Labeled sections were viewed with an epifluorescent microscope at ×100 magnification using an FITC filter.

(A) Vascular bundle, labeled with immune sera, showing labeling of the companion cells (cc) and phloem parenchyma (pp) of the phloem (ph). Cortical cells (co) are moderately labeled, as are vascular parenchyma cells of the xylem (x). se, sieve element.

(B) Vascular bundle similar to that shown in **(A)**, labeled with preimmune sera. No labeling is evident in phloem (ph) or cortex (c); however, autofluorescence of xylem (x) is visible.

(C) Another view of vascular bundle with immune sera, showing labeling of vascular parenchyma but not tracheary elements (x) or pith (pi).

(D) Same view of vascular bundle as **(C)** labeled with preimmune sera, showing no labeling of vascular parenchyma or pith (pi) but showing autofluorescence from xylem (x).

(E) Periphery of stem section labeled with immune sera, showing intense labeling of guard cells (gc) and moderate labeling of cortical cells (co).

(F) Outer edge of stem section labeled with preimmune sera, showing no labeling of guard cells (gc) or cortical cells.

(G) through **(I)** show leaf veins, either major veins in **(G)** and **(I)** or minor veins in **(H)**.

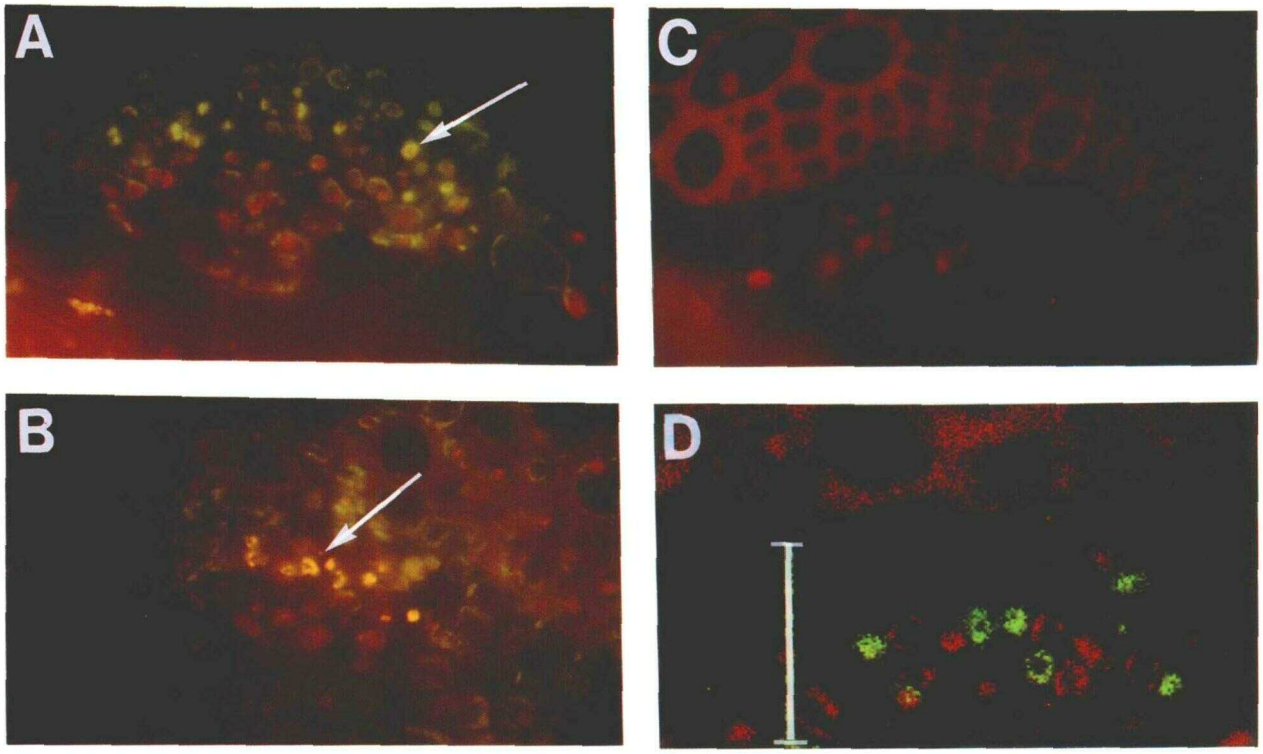

Figure 9. Arabidopsis Stem Vascular Bundle Stained with Various Combinations of Anti–c-Myc and Anti–H^+-ATPase Immune and Preimmune Sera.

(A) Stem transection from plant expressing AHA3–c-Myc, labeled with anti–H^+-ATPase immune sera and FITC-conjugated secondary antibody, viewed with double-band pass filter specific for both FITC and rhodamine red. All plasma membrane labeling of phloem cells appears green, including companion cells (arrow).

(B) Another stem transection from a plant expressing AHA3–c-Myc, labeled with both anti–H^+-ATPase immune and anti–c-Myc sera, detected with FITC- and rhodamine red–conjugated secondary antibodies, respectively, and viewed with double-band pass filter. Phloem parenchyma, vascular parenchyma, and cambial cells appear green, whereas companion cells appear yellow-orange (arrow).

(C) Stem transection from untransformed control plant, labeled with anti–H^+-ATPase preimmune and anti–c-Myc sera, detected with FITC-and rhodamine red–conjugated secondary antibodies, respectively, and viewed with double-band pass filter. Only autofluorescence from xylem and chloroplasts is evident.

(D) Distribution of a sieve element–specific antigen and AHA3–c-Myc in vascular bundles. Arabidopsis stems were double labeled with RS5 (anti–β-amylase) and anti–c-Myc sera, and detected with rhodamine red– and FITC-conjugated secondary antibodies, respectively. An image at the excitation wavelength corresponding to each fluorochrome was collected using a laser confocal microscope in the dual channel mode (λ = 488 nm for FITC and 568 nm for rhodamine red). Images were digitized and merged, assigned pseudocolors denoting rhodamine red (red) and FITC (green), and contrast stretched using the Bio-Rad Cosmos imaging program. RS5 is shown labeling the periphery of sieve elements (red), and anti–c-Myc is shown labeling the periphery of adjacent companion cells (green). **(A)** to **(C)** are at half the magnification of **(D)**. Bar = 10 μm and shows location of phloem.

observation reflects a passive role in establishing the proton motive force that drives the sucrose carriers that mediate phloem loading. It is perhaps unsurprising that this highly specialized ancillary cell type, which is devoid of organelles such as nuclei and Golgi complexes, has relinquished its role in active membrane transport and serves simply as a conduit, as its streamlined morphology implies. Because of the high speed and volume with which solutes flow through the sieve tube, the H^+-ATPases' requirement for high levels of ATP may have necessitated their partitioning into companion cells, where ATP can accumulate without being swept away in the transport stream.

It may be important to note that due to extensive plasmodesmata connections (Evert, 1990; Lucas and Wolf, 1993) between the companion cell and sieve tube elements, a highly negative electric potential generated by the proton pump in the companion cell would be instantaneously transferred to the sieve tube cell. Hence, although the sieve element plasma membrane may be devoid of ATPase, it could nevertheless maintain a high electric potential and thus be capable of driving

the influx of sugars directly from the apoplast without a contribution from the companion cell (see Figure 10). Studies localizing the proton-coupled sugar carriers, similar to those performed in this study with the ATPase protein, are needed to test this idea. In a recent study using a monospecific polyclonal antibody, one isoform of the gene family encoding the plasma membrane sucrose carrier was immunocytochemically localized in companion cells, but not sieve elements, within the phloem of petioles from *Plantago major* (Stadler et al., 1995). It remains to be established whether other isoforms of the sucrose carrier gene family are similarly absent from sieve elements.

Immunolocalization approaches avoid potential artifacts inherent with β-glucuronidase/promoter fusion studies (Plegt and Bino, 1989; Mascarenhas and Hamilton, 1992; Uknes et al., 1993) and offer improved resolution of localizations in cellular and subcellular compartments. However, high levels of amino acid homology between AHA isoproteins have impeded generation of specific antibodies for localization studies. At least 10

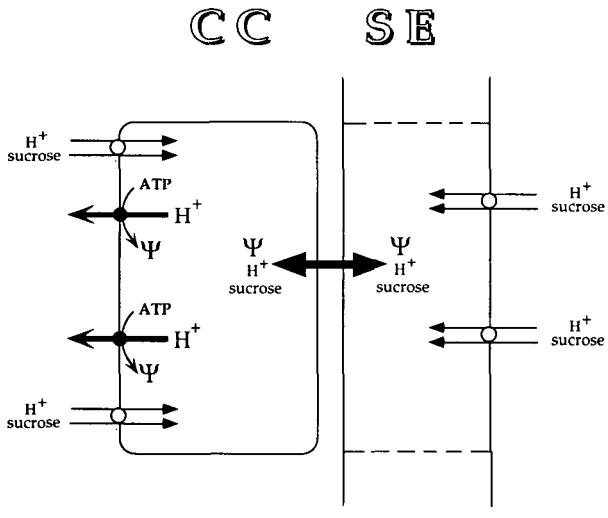

Figure 10. Model of Transport Functions Partitioned between Cells within the Phloem during Apoplastic Loading.

AHA3 proteins (closed circles) in the companion cell plasma membrane pump consume ATP and pump protons out of the cell, generating a H^+ chemical gradient and an electric potential (Ψ). This electrochemical gradient in turn is used by sucrose transporters (open circles) to load sucrose into the companion cell (CC)–sieve element (SE) complex. For long-distance transport via the sieve elements, sucrose either moves first into the companion cell and is then passively transferred through plasmodesmata (denoted by bidirectional arrow traversing the two cell types) to the sieve elements or is moved directly across the plasma membrane of sieve elements. The results of our study indicate that the proton pump is partitioned mainly in the plasma membrane of companion cells, with little or no pump present in the plasma membrane of sieve elements. The location of sucrose carriers shown in this diagram is uncertain because it has not yet been experimentally established for all members of the sucrose carrier gene family (Stadler et al., 1995).

Arabidopsis H^+-ATPase isoforms exist (Harper et al., 1994), and to date, only five of those have been fully cloned and sequenced. Until the complete sequence of the remaining isoforms is available, it is difficult to ensure the design of AHA3-specific antisera. Moreover, potentially isoform-specific antisera cannot be tested for cross-reactivity with the other isoforms until full-length clones are available.

There are several advantages to using epitope tagging as a means of unambiguously determining the cellular and subcellular location of AHA3. First, epitope tagging added only 16 (904 construct) or 22 (944 construct) amino acids, which likely had minimal impact on transcriptional, translational, and post-translational regulation. As a precaution, AHA3 was tagged at two positions, and the consistency of cellular localization was confirmed in multiple transgenic lines expressing both constructs. Second, tagging all AHAs with c-Myc will provide a standard for future localization studies and will eliminate variations in antisera affinities. Third, specificity of labeling was unambiguously confirmed using untransformed wild-type tissue as a genetically negative control.

The role for multiple plant plasma membrane H^+-ATPase isoproteins is unknown. One explanation is that the different genes encoding these isoproteins have evolved genetic control mechanisms for independently modulating levels of H^+-ATPase protein during differentiation. For example, the promoter for one isoform might contain the transcription machinery to specify extremely high levels of H^+-ATPase expression needed for guard cell function but not the low levels needed in adjacent epidermal cells. Another explanation for multigene families is that different AHA isoproteins possess regulatory or kinetic differences and are uniquely suited to the physiological needs of various tissues. This latter possibility was recently supported by evidence for differences in the kinetic and regulatory properties of AHA1, AHA2, and AHA3 isoproteins expressed in yeast (Palmgren and Christensen, 1994).

In conclusion, this study indicates that AHA3 is specifically expressed in the plasma membrane of phloem companion cells. Overall H^+-ATPase content in different cell types appears to vary, depending on the cell's transport activity, whereas AHA3 expression is always restricted to companion cells and seems unaffected by the physiological and developmental demands of surrounding tissue. For example, AHA3 expression in fully expanded leaves, which are specialized for massive photoassimilate export, was not appreciably higher than in stems, which, as essentially nonphotosynthetic tissues, are not expected to be similarly engaged.

Now that the specific localization of AHA3–c-Myc in companion cell plasma membrane has been determined, subcellular fractionation may provide a means of separating vesicles containing AHA3–c-Myc from other cellular membranes, thus isolating companion cell plasma membranes from heterogeneous membrane preparations. For example, immunological affinity purification procedures could be used to isolate companion cell plasma membrane vesicles containing AHA3–

c-Myc, which could then be used to identify companion cell–specific membrane proteins and biochemical activities. In addition, epitope tagging other *AHA* gene isoforms expressed in a variety of cell types could help to identify plasma membrane vesicle populations from different cell types, thus clarifying a source of ambiguity and heterogeneity in membrane fractionation and biochemical analyses. Extending this analysis to other transport proteins will provide valuable tools for dissecting and analyzing functionally distinct membrane transport proteins that were previously indistinguishable using biochemical and immunocytochemical approaches. Assigning these biochemical activities to cells within the plant will provide a coherent view of plant transport that integrates membrane transport functions with cellular architecture.

METHODS

Construction of AHA3 Plasmids and Site-Directed Mutagenesis

The DNA clone λgAHA3-6, which contains Arabidopsis H^+-ATPase isoform 3 (*AHA3*) genomic sequences, was described by Harper et al. (1990). The genomic interval containing *AHA3* spans ~12 kb and was subcloned in two pieces into pBluescript SK– (Stratagene, LaJolla, CA). The plasmid containing the 9-kb SpeI fragment (4 kb of 5′ flanking sequences and 5 kb of genomic coding sequences) was designated pgAHA3S. The plasmid containing the 3-kb XbaI-SalI fragment (3′ end of the coding region and 2.3 kb of 3′ flanking sequences) was designated pgAHA3-3′SX.

5′ and 3′ flanking and coding sequences of *AHA3* were cloned into the plant expression vector pBIN19 (Bevan, 1984) in multiple steps. First, the 4.4-kb XbaI-SalI fragment from pgAHA3-3′SX was cloned into the XbaI-SalI sites of pBIN19. The resulting plasmid was designated pBIN3′XS. The 2.4-kb SpeI-XbaI fragment of this plasmid was replaced with the 9-kb SpeI fragment from pgAHA3S. The resulting plasmid, pBIN:3S, contained ~12 kb of *AHA3* genomic sequence, including all coding sequences and 5′ and 3′ flanking sequences. This plasmid was later used to introduce the epitope tags into the *AHA3* coding sequence and for Arabidopsis transformation.

A ClaI deletion of pgAHA3S was generated, leaving the 2.7-kb 3′ portion of the clone. This fragment, designated p3SCla, was used for site-directed mutagenesis to introduce BamHI sites at nucleotide positions 5180 and 5370, using the *dut⁻ ung⁻* method (Kunkel et al., 1987). The degenerate mutagenesis oligonucleotides 2BM 903 (ATCTCAGGATCCTCTCTGTAAC[C/T][A/T]CCT) and 2BM 944 (GTGGGGATCCG[C/G][T/A]GT[T/C/A]TCAATGTC) contained nucleotide substitutions to introduce BamHI sites at nucleotides encoding amino acids 904 and 944, respectively (degenerate nucleotides are indicated by parentheses). Using reagents in the Muta-Gene Phagemid *In Vitro* Mutagenesis Kit v.2 (Bio-Rad), single-stranded DNA templates of the p3SCla clone were prepared from a *dut⁻ ung⁻* RZ1032 strain followed by superinfection by M13K07 helper phage. Oligonucleotides 2BM903 and 2BM944 were phosphorylated and annealed to the single-stranded template. T7 DNA polymerase was used to prime synthesis of the complementary strand from the mutagenesis primers, and the plasmid was circularized with T4 DNA ligase. Mutant plasmids containing the new BamHI sites were then propagated and designated p3SCla-904 and p3SCla-944.

Construction of c-Myc-Tagged *AHA3* Clones

Single-stranded complementary oligonucleotides for the c-Myc epitope (coding strand, 5′-AAGGATCCTCCGGAGCAAAAGCTTATCAGTGAG-3′; noncoding strand, 5′-GAAGCTATAGCAACTGCTTCTCTCATAGA-3′) were annealed, and complementary strands were synthesized with Klenow. The double-stranded primers were phenol–chloroform extracted, ethanol precipitated, digested with BamHI and BglI, and ligated into the BamHI site of p3SCla-904 and p3SCla-944 (introduced by site-directed mutagenesis as described above). Clones were sequenced to confirm correct orientation and fusion sequences. Sequencing revealed that all 944 clones were missing two nucleotides, which resulted in the loss of the termination codon, changed the last two amino acids, and added three amino acids to the end (i.e., planned sequence, CTAGATCCCCACACCGTT**TAA**TAA; observed sequence with deletion, CTAGATCCCCACCGTTTAATAAATATT**TAA**; deleted nucleotides are underlined, stop codons are in bold).

The 904 clones were sequenced from a PmlI site (nucleotide 4542) to a HpaI site (nucleotide 5270), and 944 clones were sequenced from a HpaI site (nucleotide 5270) to an SpeI site (nucleotide 5719) to confirm that there were no errors introduced by the site-directed mutagenesis procedure. The 904 clones' HpaI-PmlI fragment and the 944 clones' HpaI-SpeI fragment, each containing epitope tag sequences, were then cloned back into parental p3SCla, replacing the native sequences.

Sequences at the fusion sites are as follows, with native *AHA3* sequences in italics, BamHI and BamHI-BglII sites underlined, and c-Myc epitope sequences in bold: 904 *AHA3–myc*, *GGT GGT TAC AGA* GAG GAT CCT CCG GAG **CAA AAG CTTATC AGT GAG GAA GAC TTG** CTAGAT CCT *GAG ATT*; 944 *AHA3–myc*, *GAC ATT GAG ACA* GCG GAT CCT CCG GAG **CAA AAG CTTATC AGT GAG GAA GAC TTG** CTA GAT CCC CAC CGT TTAATA AAG ATT.

For the final construction, the ClaI-SpeI fragments, now containing the epitope tags, were cloned into pBIN:gAHA3, which had been linearized with SpeI, then partially digested with ClaI, thus replacing the native sequences spanning the ClaI-SpeI sites with ones containing epitope tags. To confirm that sites had not been deleted during this procedure, the native pBIN19 and pgAHA3S clones were digested with the various four base cutters and electrophoretically analyzed to account for all fragments. Agrobacterium and Arabidopsis transformations were conducted as described by DeWitt et al. (1991).

Antibodies

Anti-H^+-ATPase polyclonal antibodies were generated against a fusion protein of the AHA2 C terminus and glutathione *S*-transferase protein (N.D. DeWitt, M.R. Sussman, and J.F. Harper, unpublished data). Antisera for immunolocalizations were precleared against glutathione *S*-transferase. Monoclonal RS5 (anti-β-amylase, IgM) was the kind gift of R. Sjölund (University of Iowa, Iowa City). Anti-c-Myc monoclonal 9E10.2 was obtained from Oncogene Science (Manhasset, NY). Sources of fluorochrome-conjugated secondary antibodies were as follows: rabbit anti-mouse IgG_1 fluorescein, Cappell (Durham, NC); goat anti-mouse IgG_1 rhodamine red, Southern Biotechnology Associates (Birmingham, AL); goat anti-rabbit IgG fluorescein, Cappell; affinity-purified goat anti-mouse IgM fluorescein, Cappell; and goat anti-mouse IgM rhodamine, Sigma.

Microsomal Protein Preparation for Immunoblot

All manipulations were conducted on ice or in a cold room, with prechilled buffers. Arabidopsis plants were grown under continuous light on solid Murashige and Skoog media (Sigma) containing kanamycin (50 mg/mL) or no kanamycin for wild-type control plants. Whole plants were frozen in liquid nitrogen and then ground in a mortar with a pestle. Extraction buffer containing 290 mM sucrose, 25 mM EDTA, 250 mM Tris, pH 8.5, 2 mM phenylmethyl sulfonyl fluoride, and 76 mM β-mercaptoethanol was added to ground tissue (2 mL/g wet weight). Tissue was homogenized with five passes of a Teflon (Du Pont) glass homogenizer, and the homogenate was spun for 5 sec in a microcentrifuge to remove cell wall material and large debris. After repeating this step once, supernatant was transferred to a fresh tube and centrifuged for 1 hr. The microsomal pellet was suspended in fresh extraction buffer, and protein concentrations were determined (Lowry et al., 1951).

Immunoblotting

Samples were solubilized by incubating for 15 min at 25°C in 3 × solubilization buffer (100 mM Tris, pH 6.8, 3.7% [w/v] SDS, 5% [w/v] DTT, 20% [w/v] sucrose, 0.3% [w/v] bromphenol blue). After separating proteins by SDS-PAGE on 8% (w/v) (for anti–H+-ATPase blot) or 6% (w/v) (for 9E10.2 blot) acrylamide gels, proteins were transferred to Immobilon-P polyvinylidene difluoride membranes (Millipore), using a Hoefer Transphor apparatus (Hoefer Scientific Instruments, San Francisco, CA), at 500 mA for 12 hr, at 4°C. Transfer buffer consisted of 192 mM glycine, 25 mM Tris-base, and 0.02% (w/v) SDS.

The blot was blocked overnight in 20 mM Tris, pH 7.6, 137 mM NaCl, 0.1% (v/v) Tween 20 (TBS-T) with 5% (w/v) nonfat dry milk. Primary antiserum dilutions were as follows: anti–H+-ATPase CTF, 1:2000; and anti–c-Myc 9E10.2, 1:2000. For 9E10.2 immunoblots, an intermediate antiserum incubation step was included: rabbit anti–mouse IgG, 1:2000; 1-hr incubation, followed by four washes for 15 min each in TBS-T. Goat anti–rabbit horseradish peroxidase–conjugated secondary antibody (Amersham) was diluted to 1:2000 in blocking buffer. Primary and secondary incubations were for 1 hr at room temperature and were followed by four washes for 15 min each in TBS-T. ECL chemiluminescent reagents (Amersham) were used for detection.

Indirect Immunofluorescence

Stem sections (~100 to 500 μm) were handcut using Teflon (Du Pont) razor blades (Ted Pella, Redding, CA). Sections were either used immediately or fixed for 1 hr in 4% (w/v) paraformaldehyde and 50 mM sodium phosphate, pH 7.2. Rosette leaves were embedded in TFM freezing medium (Fisher Scientific) and frozen with Histo-Freeze 22 aerosol spray (Fisher Scientific). Eight-micron sections were cut with a cryostat, collected on poly-L-lysine–coated slides, and stored at 4°C. Before immunostaining, slides containing leaf sections were incubated for 5 min in PBS to remove freezing medium.

Sections were blocked for 45 min in 2.5% (w/v) nonfat dry milk, 10% (v/v) normal serum in PBS. Dry milk solution was warmed to 60°C and centrifuged before use. Blocking serum was from the animal species that produced secondary antibody. For immunofluorescence, antibodies were diluted in blocking buffer at the following concentrations: 9E10.2, 1:5; H+-ATPase polyclonal, 1:20; and RS5, 1:1000. Sections were incubated for 1 hr in primary antisera diluted in blocking buffer, then washed three times for 15 min each in PBS. Secondary antisera were diluted in blocking buffer at 1:100. Sections were incubated in diluted secondary antibodies for 1 hr, followed by three washes for 15 min each in PBS.

Immunostained sections were mounted in 90% (v/v) glycerol, 10% (v/v) PBS, containing 0.2% (w/v) *p*-phenyldiamine to prevent photobleaching. For epifluorescent microscopy, samples were observed on an inverted microscope (Nikon, Melville, NY), using fluorescein isothiocyanate (FITC), rhodamine red, or double FITC/rhodamine red filters (Fryer Company, Huntley, IL). Some samples were also examined for immunofluorescence using a laser scanning confocal microscope (model MRC-600; Bio-Rad) equipped with a filter for reducing chloroplast autofluorescence (SWP filter 935; Reynard Enterprises, Laguna Niguel, CA).

Controls for Immunofluorescence Labeling Specificity

As controls for polyclonal anti–H+-ATPase labeling, sections were incubated with preimmune sera (cleared against glutathione *S*-transferase) and with secondary antibodies alone. As controls for 9E10.2 labeling, antibody incubations were performed simultaneously on sections from untransformed control plants. For epifluorescent and confocal double-labeling experiments, absence of signal bleed-through was confirmed by examining single-labeled samples using individual wavelength filters.

Tissue Preparation for Standard Electron Microscopy

Arabidopsis thaliana (ecotype Bensheim) was grown in pots for 8-hr day lengths. Rosette leaves and bolting stems were submerged in 100 mM sodium phosphate buffer, pH 7, and cut into ~1-mm-wide pieces. Tissue was fixed in 3% (v/v) glutaraldehyde, 100 mM sodium phosphate, pH 7, for 4 hr, and then washed four times for 15 min each in 100 mM sodium phosphate, pH 7, and postfixed in 1% (v/v) OsO_4 overnight at 4°C. After three washes of 5 min each in 100 mM sodium phosphate, pH 7, tissue was dehydrated through an acetone series (10, 30, 50, 70, and 90%) for 15 min each, followed by two washes with 100% acetone for 30 min each. Tissue was infiltrated with Spurr's resin as follows: 1:2 Spurr's, acetone, overnight; 2:1 Spurr's, acetone, 2 hr; and 100% Spurr's, three times for 2 hr each. Tissue was placed in freshly mixed Spurr's resin and cured in a vacuum oven at 70°C overnight. Silver–gold sections were collected on Formvar-coated slot grids or uncoated copper grids. Sections were poststained with 2% (w/v) uranyl acetate (aqueous) for 30 min at 37°C, followed by alkaline lead citrate for 10 min at room temperature. Specimens were observed with an electron microscope (Model 410; Philips Electronic Instruments, Mahwah, NJ).

Tissue Preparation for Immunogold Labeling

A. thaliana (ecotype Bensheim) was grown in pots for 8-hr daylengths. Bolting stems from 3- to 6-week-old plants were submerged in 50 mM phosphate buffer, pH 7, and cut into ~1-mm-wide pieces. Tissue was fixed in 4% (w/v) paraformaldehyde, 100 mM sodium phosphate, pH 7, for 4 hr, then washed four times for 15 min each in 100 mM sodium phosphate, pH 7. Tissue was then dehydrated through an ethanol series: 30, 50, 70, and 90%, then two times with 100% ethanol for 15 min each. The 30% ethanol was at 4°C, and all other steps were at

−20°C. Tissue was then infiltrated with Lowicryl, also at −20°C: 1:1 ethanol, Lowicryl; 1:2 ethanol, Lowicryl; and 100% Lowicryl. Samples were kept in 100% Lowicryl for 5 days, changing to fresh resin each day. Resin was polymerized with UV light for 2 days at −20°C and then for 1 day at room temperature. Silver–gold sections were collected on Formvar-coated nickel grids and immunolabeled.

Immunogold Labeling

Nonspecific binding sites were blocked for 15 min with 5% (w/v) nonfat dry milk, 0.1% (w/v) BSA, in TBS-T (20 mM Tris, pH 7, 500 mM NaCl, 0.5% [v/v] Tween 20) and then for 15 min with 5% (v/v) normal goat serum in TBS-Tween. Polyclonal anti-H^+-ATPase immune and preimmune sera (cleared) were diluted 1:10 in 5% goat serum/TBS-T and incubated overnight at 4°C. Grids were washed in TBS-T five times for 5 min each. Grids were then incubated for 1 hr in goat anti-rabbit IgG–15-nm gold conjugate (Ted Pella), diluted 1:25 in 5% (v/v) goat serum in TBS-T. Grids were washed two times for 5 min each in TBS-T and three times for 5 min each in double-distilled H_2O. Sections were poststained in 2% (w/v) uranyl acetate for 30 min at 37°C and observed with a Philips 410 electron microscope.

ACKNOWLEDGMENTS

We thank Dr. Richard Sjölund for help with immunofluorescence and Dr. Ray Evert for assistance in identifying phloem cell types and use of his microscopic facilities. We are grateful to Dr. Bill Russin and Renate Bromberg for training in electron microscopy; to Dr. Jeffrey F. Harper for the degenerate mutagenesis primers; and to Dr. Jeffrey Young, Dr. Fernando Camilo, and Jennifer Gottwald for critical reading of the manuscript. This research was supported by grants from the Department of Energy/National Science Foundation/United States Department of Agriculture Collaborative Program in Plant Biology (No. BIR 92-20331) and from the Department of Energy (No. DE-F602-88ER13938).

Received July 7, 1995; accepted October 9, 1995.

REFERENCES

Bevan, M. (1984). Binary *Agrobacterium* vectors for plant transformation. Nucleic Acids Res. **12,** 8711–8721.

Bouche-Pillon, S., Fleurat-Lessard, P., Fromont, J.-C., Serrano, R., and Bonnemain, J.-L. (1994). Immunolocalization of the plasma membrane H^+-ATPase in minor veins of *Vicia faba* in relation to phloem loading. Plant Physiol. **105,** 691–697.

Boutry, M., Michelet, B., and Goffeau, A. (1989). Molecular cloning of a family of plant genes encoding a protein homologous to plasma membrane H^+-translocating ATPases. Biochem. Biophys. Res. Commun. **162,** 567–574.

Bush, D.R. (1993). Proton-coupled sugar and amino acid transporters in plants. Annu. Rev. Plant Physiol. Plant Mol. Biol. **44,** 513–542.

DeWitt, N.D. (1994). Epitope Tagging and Reporter Gene Studies Identify an Arabidopsis Plasma Membrane Proton Pump Specific for Phloem Companion Cells. PhD dissertation (Madison, WI: University of Wisconsin).

DeWitt, N.D., Harper, J.F., and Sussman, M.R. (1991). Evidence for a plasma membrane proton pump in phloem cells of higher plants. Plant J. **1,** 121–128.

Evert, R.F. (1990). Dicotyledons. In Sieve Elements—Comparative Structure, Induction, and Development, H.-D. Behnke and R.D. Sjolund, eds (Berlin: Springer-Verlag), pp. 103–137.

Ewing, N.N., and Bennett, A.B. (1994). Assessment of the number and expression of P-type H^+-ATPase genes in tomato. Plant Physiol. **106,** 547–557.

Ewing, N.N., Wimmers, L.E., Meyer, D.J., Chetelat, R.T., and Bennett, A.B. (1990). Molecular cloning of tomato plasma membrane H^+-ATPase. Plant Physiol. **94,** 1874–1881.

Harper, J.F., Surowy, T.K., and Sussman, M.R. (1989). Molecular cloning and sequence of cDNA encoding the plasma membrane proton pump (H^+-ATPase) of *Arabidopsis thaliana.* Proc. Natl. Acad. Sci. USA **86,** 1234–1238.

Harper, J.F., Manney, L., DeWitt, N.D., Yoo, M.H., and Sussman, M.R. (1990). The *Arabidopsis thaliana* plasma membrane $H(^+)$-ATPase multigene family: Genomic sequence and expression of a third isoform. J. Biol. Chem. **265,** 13601–13608.

Harper, J.F., Manney, L., and Sussman, M.R. (1994). Evidence for at least ten plasma membrane H^+-ATPase genes in *Arabidopsis*, and complete genomic sequence of AHA10 which is expressed primarily in developing seeds. Mol. Gen. Genet. **244,** 572–587.

Houlné, G., and Boutry, M. (1994). Identification of an *Arabidopsis thaliana* gene encoding a plasma membrane H^+-ATPase whose expression is restricted to anther tissue. Plant J. **5,** 311–317.

Katz, D.B., Sussman, M.R., Mierzwa, R.J., and Evert, R.F. (1988). Cytochemical localization of ATPase activity in oat roots localizes a plasma membrane–associated soluble phosphatase, not a proton pump. Plant Physiol. **86,** 841–847.

Kolodziej, P., and Young, R.A. (1991). Epitope tagging and protein surveillance. Methods Enzymol. **194,** 508–519.

Kunkel, T.A., Roberts, J.D., and Zakour, R.A. (1987). Rapid and efficient site-specific mutagenesis without phenotypic selection. Methods Enzymol. **154,** 367–382.

Lowry, O.H., Rosebrough, N.J., Farr, A., and Randall, R.J. (1951). Protein measurement with the Folin phenol reagent. J. Biol. Chem. **193,** 265–275.

Lucas, W.J., and Wolf, S. (1993). Plasmodesmata: The intercellular organelles of green plants. Trends Cell Biol. **3,** 308–315.

Mascarenhas, J.P., and Hamilton, D.A. (1992). Artifacts in the localization of GUS activity in anthers of petunia transformed with a CaMV 35S-*GUS* construct. Plant J. **2,** 405–408.

Monk, B.C., Montesinos, C., Ferguson, C., Leonard, K., and Serrano, R. (1991). Immunological approaches to the transmembrane topology and conformational changes of the carboxyl-terminal regulatory domain of yeast plasma membrane H^+-ATPase. J. Biol. Chem. **266,** 18097–18103.

Obermeyer, G., Lützelschwab, M., Heumann, H.G., and Weisenseel, M.H. (1992). Immunolocalization of H^+-ATPases in the plasma membrane of pollen grains and pollen tubes of *Lilium longiflorum.* Protoplasma **171,** 55–63.

Palmgren, M.G., and Christensen, G. (1993). Complementation in situ of the yeast plasma membrane H^+-ATPase *pma1* by an H^+-ATPase gene from a heterologous species. FEBS Lett. **317,** 216–222.

Palmgren, M.G., and Christensen, G. (1994). Functional comparisons between plant plasma membrane H+-ATPase isoforms expressed in yeast. J. Biol. Chem. **269,** 3027–3033.

Pardo, J.M., and Serrano, R. (1989). Structure of a plasma membrane H+-ATPase gene from the plant *Arabidopsis thaliana.* J. Biol. Chem. **264,** 8557–8562.

Parets-Soler, A., Pardo, J.M., and Serrano, R. (1990). Immunocytolocalization of plasma membrane H+-ATPase. Plant Physiol. **93,** 1654–1658.

Plegt, L., and Bino, R.J. (1989). β-Glucuronidase activity during development of the male gametophyte from transgenic and nontransgenic plants. Mol. Gen. Genet. **216,** 321–327.

Samuels, A.L., Fernando, M., and Glass, D.M. (1992). Immunofluorescent localization of plasma membrane H+-ATPase in barley roots and effects of K+ nutrition. Plant Physiol. **99,** 1509–1514.

Serrano, R. (1989). Structure and function of plasma membrane ATPase. Annu. Rev. Plant Physiol. Plant Mol. Biol. **40,** 61–94.

Serrano, R., Monk, B.C., Villalba, J.M., Montesinos, C., and Weiler, E.W. (1993). Epitope mapping and accessibility of immunodominant regions of yeast plasma membrane H+-ATPase. Eur. J. Biochem. **212,** 737–744.

Stadler, R., Brandner, J., Schulz, A., Gahrtz, M., and Sauer, N. (1995). Phloem loading by the PmSUC2 sucrose carrier from *Plantago major* occurs into companion cells. Plant Cell **7,** 1545–1554.

Stenz, H.-G., Heumann, H.-G., and Weisenseel, M.H. (1993). High concentration of plasma membrane H+-ATPase in root caps of *Lepidium sativum* L. Naturwissenschaften **80,** 317–319.

Sussman, M.R. (1994). Molecular analysis of proteins in the plant plasma membrane. Annu. Rev. Plant Physiol. Plant Mol. Biol. **44,** 253–281.

Uknes, S., Dincher, S., Friedrich, L., Negrotto, D., Williams, S., Thompson-Taylor, H., Potter, S., Ward, E., and Ryals, J. (1993). Regulation of pathogenesis-related protein-1a gene expression in tobacco. Plant Cell **5,** 159–169.

Villalba, J.M., Liitzelschwab, M., and Serrano, R. (1991). Immunocytolocalization of plasma-membrane H+-ATPase in maize coleoptiles and enclosed leaves. Planta **185,** 458–461.

Wang, Q., Monroe, J., and Sjolund, R.D. (1995). Identification and characterization of a phloem-specific β-amylase. Plant Physiol. **109,** 743–750.